Some Observations on the Relationship Between the Effects of Pressure Upon the Fracture Mechanisms and the Ductility of Fe-C Materials

Thomas E. Davidson and George S. Ansell

It has been known for a considerable period of time that the ductility of even quite brittle materials can be enhanced if they are deformed under a superposed hydrostatic pressure of sufficient magnitude. The response of ductility to pressure, however, has been shown to vary considerably between materials. Prior work has shown that the effects of pressure upon the tensile ductility of Fe-C materials depend upon the amount, shape and distribution of the brittle cementite phase. In this current investigation, the effects of pressure upon the fracture mechanisms in a series of annealed and spheroidized Fe-C materials were examined. It was observed that the principal effect of pressure is to suppress void growth and coalescence, retard cleavage fracture and to enhance the ductility of cementite platelets in pearlite. Based upon the observed effects of pressure upon the fracture mechanisms, a proposed explanation for the enhancement in ductility by pressure and for the structure sensitivity of the phenomena is presented and discussed.

THE effect of superposed pressure upon the tensile ductility of a variety of metals has been well documented.[1-12] Some of the results from several investigators are summarized in Fig. 1 where tensile ductility in terms of true strain to fracture (ϵ_f) is plotted as a function of the superposed pressure. As can be seen, a pressure of sufficient magnitude can significantly enhance the ductility of metals. However, Fig. 1 also demonstrates that the response of ductility to pressure and the form of the ductility-pressure relationship varies considerably between materials.

Several explanations have been offered for the observed enhancement in ductility by a superposed pressure. Although no experimental evidence was provided, Bridgman[13] and Bobrowsky[10] proposed that the observed effect was due to the prevention or healing of microcracks or holes. Bulychev *et al.*[14] observed that cracks and voids in initially prestrained copper were healed in the necked region of a tensile specimen upon further straining while under a superposed pressure. Also, Pugh[5] observed that large cavities were suppressed in copper fractured in tension while under pressure.

A second proposal has been forwarded by Beresnev *et al.*[6] This proposal is based upon the hypothesis that a material fails in a brittle manner because the normal tensile stress reaches a critical value before the shear stress is of sufficient magnitude to cause plastic flow. Since a superposed hydrostatic pressure will increase the ratio of shear to normal tensile stress, a sufficiently high hydrostatic pressure should favor plastic flow while retarding brittle fracture.

Galli[15] reported that a superposed pressure shifts the ductile-brittle transition temperature of molybdenum. This was explained based upon the reduction of the normal tensile stress by the superposed pressure. Pugh[5] explained the occurrence of the observed pressure induced brittle-to-ductile transition in zinc in the same manner.

Davidson *et al.*[12] proposed an explanation for the enhancement of ductility by pressure based upon the effects of pressure upon the stress-state-sensitive stages of various fracture propagation mechanisms. Basically, they proposed that pressure will retard cleavage and intergranular fracture by counteracting the required normal tensile stress or will suppress void growth. They observed suppression of intergranular fracture and void growth in magnesium by pressure.

Davidson and Ansell[16] reported ductility as a function of pressure for a series of annealed and spheroidized Fe-C alloys. Fig. 2, from this prior work, demonstrates that the effect of pressure upon ductility is structure sensitive in terms of the amount, shape and distribution of the brittle cementite phase. As shown in Fig. 2, in the absence of cementite or when the cementite is in isolated particle form (spheroidized), the ductility-pressure relationship is linear and the slope decreases with increasing carbon content. In the annealed carbon-bearing alloys wherein the cementite is in the form of closely spaced platelets (pearlite) or in the form of a continuous network along prior austenite boundaries (1.1 pct C material), ductility as a function of pressure is nonlinear (polynomial relationship) in which the slope increases with increasing pressure. At the highest pressures studied (22.8 kbars), the slope of the curves for these materials tends to approach those for the spheroidized material of the same carbon content.

In this current investigation the change in fracture mechanisms as a function of pressure for the materials shown in Fig. 2 has been examined. The possible connection between the observed effects of pressure upon the fracture mechanisms and the effect of pressure upon ductility is discussed.

THOMAS E. DAVIDSON, formerly U.S. Research Fellow, Materials Engineering Department, Rensselaer Polytechnic Institute, Troy, N.Y., is currently Chief, Physical and Mechanical Metallurgy, Watervliet Arsenal, Watervliet, N.Y. GEORGE S. ANSELL, Member AIME, is R. W. Hunt Professor of Metallurgical Engineering, Rensselaer Polytechnic Institute. Work performed in partial fulfillment of the requirements for the degree of Doctor of Philosophy.

Manuscript submitted October 16, 1968. IMD

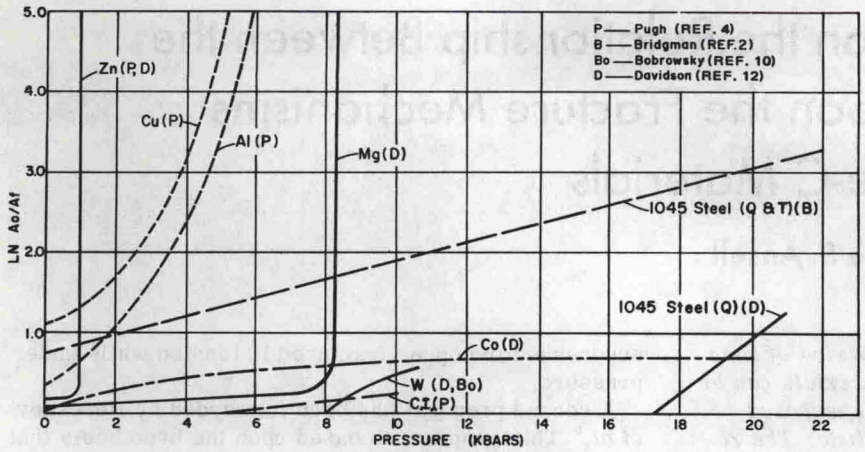

Fig. 1—Ductility vs pressure for various typical materials.

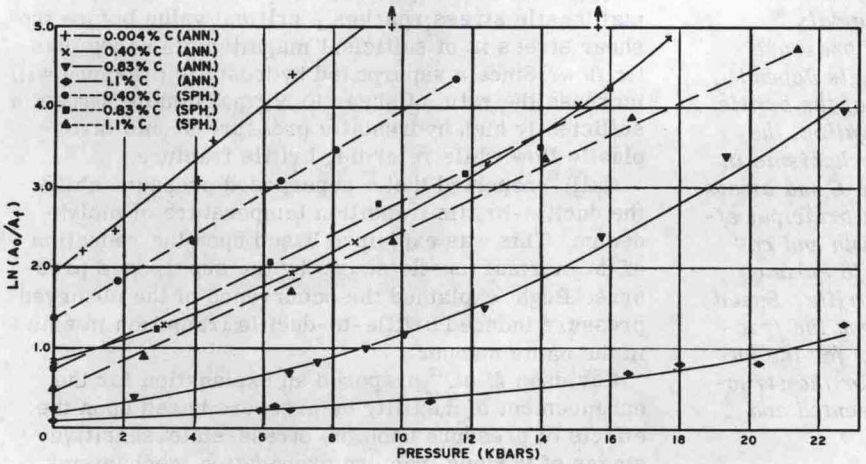

Fig. 2—Ductility vs pressure for Fe-C materials.

MATERIALS AND PROCEDURES

A) Materials. The materials used in this investigation were the same as those previously reported[16] and consisted of a series of iron-carbon alloys of the following carbon contents.

a) Fe + 0.004 pct C
b) Fe + 0.40 pct C
c) Fe + 0.83 pct C
d) Fe + 1.1 pct C

Except for the 0.004 pct C material, the materials were examined in both the spheroidized and in the annealed condition. The 0.004 pct C material was annealed only. Details of heat treatment are given in Ref. 16.

B) Procedures. The fracture appearance studies were conducted on the tensile specimens utilized in the prior work and in the development of the curves shown in Fig. 2. Additional specimens of the same materials were also examined after being strained to near fracture at various pressures in order to gain further insight into the fracture propagation process.

The high pressure tensile testing was accomplished using a Bridgman-Birch type 30 kbar hydrostatic pressure system. This system, along with the specific test procedures, was discussed in detail in previous work.[12] The tensile samples used had a 0.160 in. gage diam with a 0.665 in. gage length.

It should be noted that in the procedure used, the pressure varied by approximately 2 to 10 pct between the onset of strain of the specimen and fracture. The magnitude of the change in pressure depended upon the ductility of the material. The pressure values, shown in Fig. 2 and throughout this current work, correspond to the pressure at the point of fracture of the specimen.

The fracture appearance, from which the fracture mechanisms and their modification by pressure were deduced, was analyzed using two techniques. The first technique involved the optical examination of a longitudinal surface containing the specimen axis and intersecting the fracture surface or the necked region in the case of those specimens in which the strain was stopped just prior to total fracture. In the fractured specimens, the fracture surface was nickel plated to prevent rounding during polishing.

For the longitudinal surface examination, conventional metallographic procedures were utilized. All specimens of a given series, *i.e.*, fractured at various pressures, were polished simultaneously using an automatic polisher. To reduce the amount of flowed metal, which is particularly troublesome in void and microcrack studies, the final polishing step consisted of using 1 μ diamond paste and a hard nylon polishing cloth. The samples were ultrasonically cleaned in alcohol between each of the grinding and polishing steps.

The second examination technique involved the study of the fracture surface using electron fractography. A standard two-stage replication technique was used with 45 deg chromium shadowing.

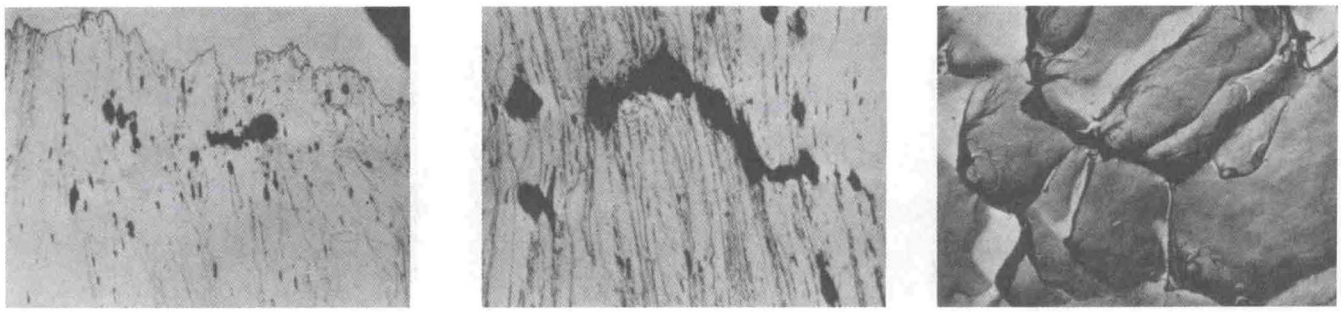

$\epsilon_f = 1.96$ (*a*) $P = 0.001$ kb $\epsilon = 1.65$ (*b*) $\epsilon_f = 1.96$ (*c*) ⊢5 μ⊣

Fig. 3—Fracture in annealed 0.004 pct C material at atmospheric pressure. (*a*) and (*b*) magnification 106 times.

RESULTS

The presentation of the results will be divided into two categories consisting of 1) annealed 0.004 pct C and spheroidized materials and 2) annealed 0.40, 0.83, and 1.1 pct C materials.

1) Fracture in Annealed 0.004 pct C and Spheroidized Materials. a) *0.004 pct C Material.* Optical and electron fractographs of the 0.004 pct C material tested at atmospheric pressure are shown in Fig. 3. As can be seen in Figs. 3(*a*) and 3(*b*), the latter of which is a specimen strained to near fracture, the fracture mechanism involves the initiation, growth, and coalescence of massive voids. The major voids are limited to the center portion of the region of greatest necking where they grow and coalesce to form a major crack. In this region the electron fractograph, Fig. 3(*c*), shows equiaxed dimples corresponding to the "hills and valleys" seen in the fracture surface, Fig. 3(*a*).

The effects of pressure upon the fracture appearance are shown in Fig. 4. There is a progressive suppression of the void growth with increasing pressure as can be seen by comparing Fig. 3(*a*) with Fig. 4. At a pressure of 2.5 kbars, Fig. 4(*a*), only a few small elongated voids are in evidence. At 15.1 kbars, Fig. 4(*b*), there appears to be no discernible voids. There is a concomitant progressive change in the fracture profile from the "hill and valley" type at atmospheric pressure, Fig. 3(*a*), to primarily a series of shear steps at 2.5 kbars, Fig. 4(*a*), and finally to a flat planar shear type fracture at 15.1 kbars, Fig. 4(*b*). Due to the small cross sectional area at 15.1 kbars, it was not possible to obtain a reliable electron fractograph. However, from the appearance of the fracture surface shown in Fig. 4(*b*) and the results from the materials to be subsequently discussed, it is highly probable that the electron fractograph would be effectively featureless.

b) *Spheroidized Material.* The typical atmospheric pressure fracture appearance in the spheroidized materials is shown in Fig. 5. As can be seen, there are three distinct stages. Referring to Fig. 5(*b*), which is located just behind the fracture surface, the first stage is the fracture of the cementite particles. Second, voids form between the segments of the fractured particles. These voids grow laterally and longitudinally as the segments of the fractured particles move apart under the influence of the continued plastic strain of the ferrite matrix. Finally, as also shown in Fig. 5(*b*), the voids coalesce resulting in a

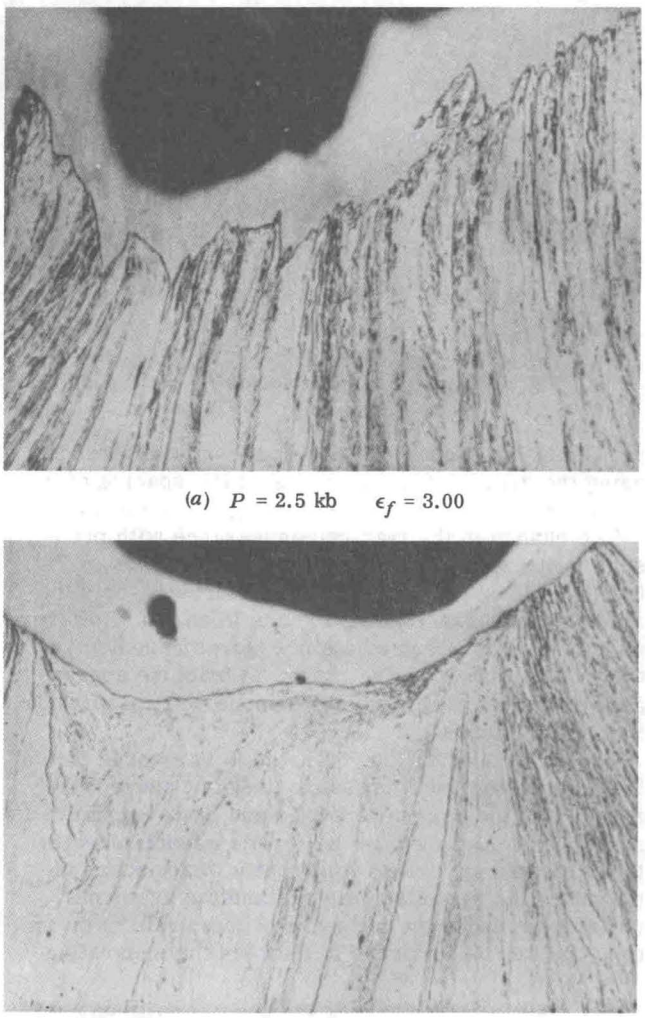

(*a*) $P = 2.5$ kb $\epsilon_f = 3.00$

(*b*) $P = 15.1$ kb $\epsilon_f > 5.0$

Fig. 4—Fracture in annealed 0.004 pct C material as function of pressure. Magnification 167 times.

major crack. These various steps in the fracture process are manifest in the fracture surface, Fig. 5(*a*), where one can see the remains of fractured cementite particles at the bottom of many "valleys". As would be expected, the electron fractograph, Fig. 5(*c*), consists of equiaxed dimples. The flat region (arrows) evident in some of the dimples in the fractograph corresponds to a fractured cementite particle.

The fracture appearance in the 0.40 and 0.83 pct C materials was effectively the same as that for the 1.1

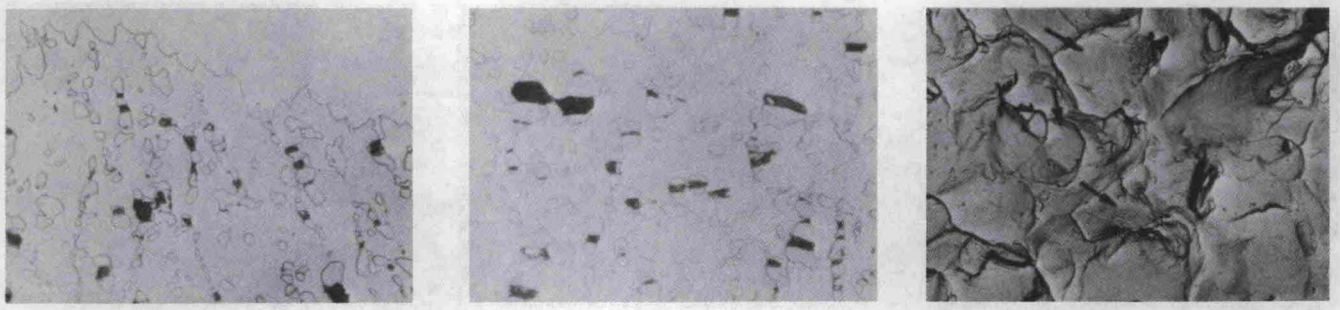

Fig. 5—Fracture in spheroidized 1.1 pct C material at atmospheric pressure. (*a*) and (*b*) magnification 530 times.

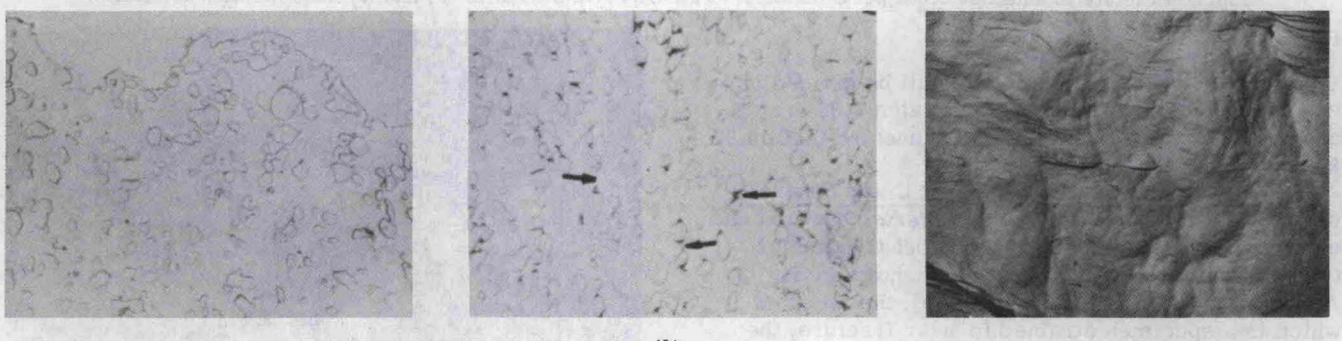

Fig. 6—Fracture in spheroidized 1.1 pct C material as function of pressure. (*a*) and (*b*) magnification 560 times.

pct C material described above, the only difference being the growth of larger voids as the spacing of the particles increased with decreasing carbon content.

The change in the fracture appearance with pressure in the spheroidized material can be seen in Fig. 6. It should be pointed out that, for brevity, only the fracture appearance at 21.3 kbars is shown. However, examination at intermediate pressures revealed that there was a progressive change in fracture appearance from that observed at atmospheric pressure to that at 21.3 kbars.

As can be seen in Fig. 6(*b*), which is an area behind the fracture surface, pressure does not prevent the fracture of the cementite particles. However, there is negligible void growth in the ferrite associated with the fractured particles. Apparently what occurs is that after the particles fracture and the segments move apart under the influence of the strain of the matrix, the ferrite is forced in between the separating segments. One can see in Fig. 6(*b*) the various stages of this process as depicted by the dark lines of varied widths connecting the two segments of fractured particles (arrows). Although it is difficult to match up the segments of a fractured particle once they are extensively separated, it appears that the ferrite surfaces between the segments are eventually forced together and rejoin.

The fracture surface, Fig. 6(*a*), shows no evidence of voids and the "hills and valleys" characteristic of fracture at atmospheric pressure. This is borne out by the electron fractograph, Fig. 6(*c*), which is effectively featureless and contains no indications of dimples or fractured cementite particles.

2) Fracture in Annealed 0.83, 0.40, and 1.1 pct C Materials. a) *Annealed 0.83 pct C Material.* The fracture appearance of this material at atmospheric pressure is shown in Fig. 7. The fracture surface, Fig. 7(*a*), consists of a series of approximately 45

Fig. 7—Fracture in annealed 0.83 pct C material at atmospheric pressure. (*a*) and (*b*) magnification 530 times.

deg facets. The various stages in the fracture process can be seen in Fig. 7(*b*) which is of an area located behind the fracture surface. First, isolated fracturing of some of those cementite platelets oriented approximately parallel to the stress direction occurs. Fracturing of the platelets then continues across the pearlite colony with the fractures lining up approximately at 45 deg to the stress direction (arrow). The second step involves the growth of voids emanating from the separation of the two parts of the fractured platelet. These voids then grow through the pearlitic ferrite and link up to form a crack across the colony. This is followed by the joining of cracks from adjacent colonies to form a major crack. Finally, this major crack grows by the continuation of this ductile pearlite fracture mechanism along with cleavage of the pearlite. The electron fractograph, Fig. 7(*c*), shows the later stages of fracture which is a mixture of long parallel dimples (arrow) characteristic of the ductile pearlite fracture process described above, and pearlite cleavage.

The effects of a superposed hydrostatic pressure of 22.8 kbars on the fracture appearance in this material are shown in Fig. 8. At this pressure the fracture surface has converted to a flat planar shear type, Fig. 8(*a*). In the region of the fracture surface, it is no longer possible to readily resolve the microstructure optically except that it consists of a series of light and dark lands. There is no evidence of pearlite cleavage or voids and associated ductile fracturing of the pearlite as was evident at atmospheric pressure.

Behind the fracture surface, Fig. 8(*b*), it can be seen that the cementite oriented parallel to the tensile direction is extensively fractured; the fractures lining up approximately along the 45 deg plane (arrow). As also shown in Fig. 8(*b*), in those pearlite colonies not oriented parallel to the tensile direction, the cementite undergoes severe bending prior to extensive fragmentation as the fracture surface is approached. Although the cementite still extensively fractures under the superposed pressure of 22.8 kbars, the pressure has imparted considerable ductility to this brittle phase as evidenced by the bending.

The electron fractograph, Fig. 8(*c*), is effectively flat and featureless showing no evidence of dimples or cleavage.

b) *Annealed 0.40 pct C Material.* The fracture appearance in the annealed 0.40 pct C hypoeutectoid steel tested at atmospheric pressure is shown in Fig. 9. As seen in Fig. 9(*a*), the fracture profile is quite ductile in appearance. Many of the "hills" or "valleys" contain pearlite.

Behind the fracture surface, Fig. 9(*b*), it can be seen that the initial stage of fracture involves fracture of the pearlite. The observed fracture process of the pearlite was the same as that previously discussed in the 0.83 pct C material (platelet fracture and void growth in the pearlitic ferrite).

The final stage of fracture in this material involves the growth and link up of voids emanating from the fractured pearlite colonies. Such voids can be seen in Fig. 9(*a*).

An electron fractograph of a pearlite-ferrite interface is shown in Fig. 9(*c*). Long parallel dimples characteristic of the ductile fracture of pearlite are in evidence (arrow). Adjacent to the pearlite fracture are portions of large dimples corresponding to the void growth in the ferrite.

The appearance of a specimen of this material fractured at a pressure of 17.6 kbars is shown in Fig. 10. At this pressure, the fracture profile, Fig. 10(*a*), is of the planar shear type. There appears to be no

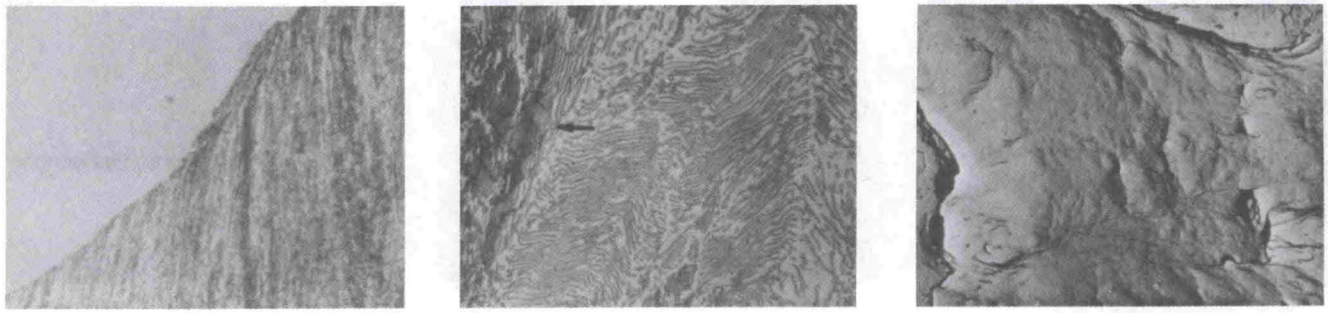

(*a*) (*b*) (*c*) ⊢5 μ⊣

Fig. 8—Fracture in annealed 0.83 pct C material at 22.8 kbars. (*a*) and (*b*) magnification 540 times.

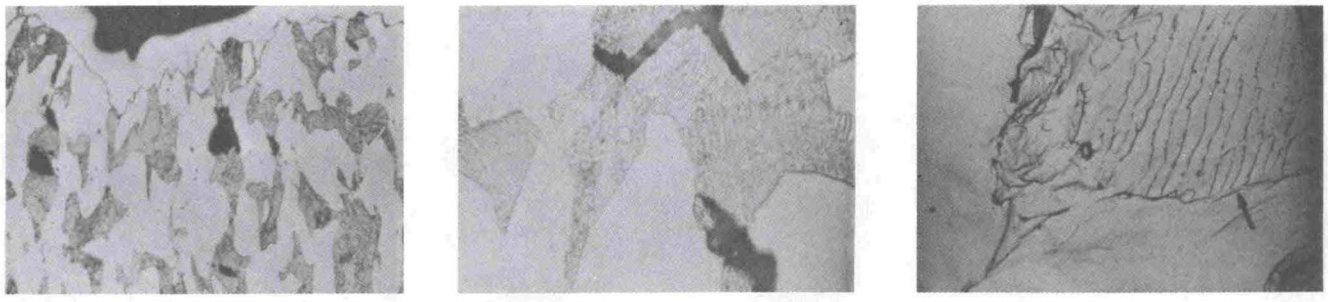

(*a*) (*b*) (*c*) ⊢5 μ⊣

Fig. 9—Fracture in annealed 0.40 pct C material at atmospheric pressure. (*a*) Magnification 106 times, (*b*) magnification 530 times.

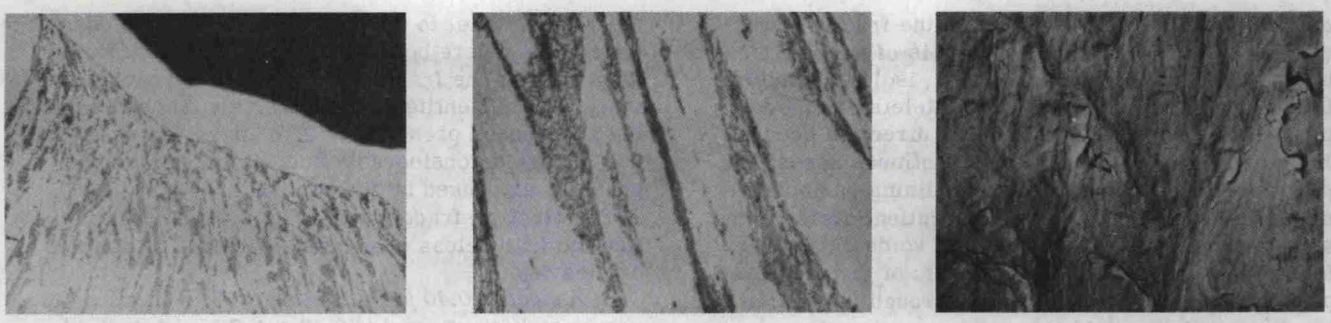

Fig. 10—Fracture in annealed 0.40 pct C material at 17.6 kbars. (*a*) Magnification 106 times, (*b*) magnification 530 times.

perturbations at the fracture surface associated with the pearlite as was the case at atmospheric pressure. As seen in Figs. 10(*a*) and (*b*) there are no voids or pearlite cracks in evidence. The cementite within the pearlite colonies, Fig. 10(*b*), is deformed and, near the fracture surface, is extensively fragmented as was the case in the eutectoid composition material. The electron fractograph, Fig. 10(*c*), reveals a fracture surface that is effectively featureless.

c) *Annealed 1.1 pct C Material.* Fracture in the annealed 1.1 pct C hypereutectoid steel at atmospheric pressure is shown in Fig. 11. As seen in Fig. 11(*a*), the fracture is generally intergranular and follows the cementite in the prior austenite boundaries. Behind the fracture surface, Fig. 6(*b*), it can be seen that the fracture occurs within the cementite at the austenite boundaries and not at the cementite-pearlite interface. Fracture of the cementite in the boundaries oriented parallel to the stress direction also occurs. However, these cracks are arrested (arrow) at the cementite-pearlite interface and do not enter into the fracture process. The electron fractograph for this material, Fig. 11(*c*), reveals a typical cleavage fracture appearance.

The effects of a pressure of 22.8 kbars on the fracture of this material are shown in Fig. 12. As seen in Fig. 12(*a*), the major portion of the fracture surface is of the planar shear type showing no discontinuities associated with the transverse or longitudinal cementite. It can also be seen that the hypereutectoid cementite is completely fragmented with the fragments (arrow) aligned parallel to the tensile stress direction. It can be seen in Fig. 12(*b*) that the fracture mode of the cementite has converted from cleavage to shear. There are no voids associated with the fragmented cementite which indicates that the pearlite may have been forced in between the separating fragments. Near the fracture surface, fracturing of the cementite within the pearlite was also observed. It appears that the hypereutectoid cementite no longer plays a role in the

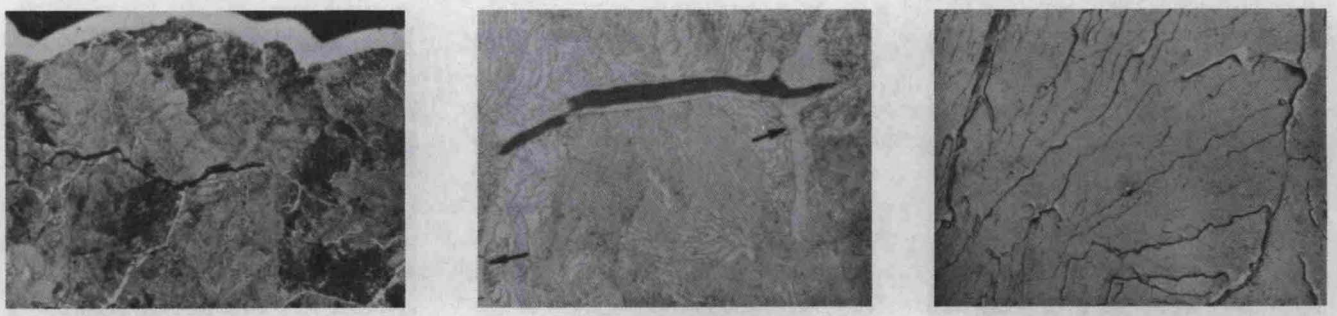

Fig. 11—Fracture in annealed 1.1 pct C material at atmospheric pressure. (*a*) Magnification 106 times, (*b*) magnification 530 times.

Fig. 12—Fracture in annealed 1.1 pct C material at 22.8 kbars. (*a*) and (*b*) magnification 530 times.

fracture process, and near the fracture surface the microstructure of this material is effectively the same as the eutectoid composition material except for the lines of cementite fragments.

The electron fractograph, Fig. 12(*c*), is again effectively featureless but does contain some isolated particles which are probably fragments of cementite particles at the fracture surface. These particles, however, do not appear to disturb the fracture surface.

DISCUSSION OF RESULTS

The fracture propagation mechanism is the same in the absence of cementite (0.004 pct C) and in the spheroidized materials and involves the growth and coalescence of isolated voids in ferrite. The spheroidized materials differ from the 0.004 pct C material only in that voids are more readily initiated (cementite particle fracture) and do not have to grow to as large a size for coalescence to occur.

The effect of pressure upon the fracture mechanism in these materials is also similar and involves the suppression of the void growth. It is important to note that the void growth suppression by the pressure is not instantaneous, but is a progressive process. This is because void growth is a shear strain process. Thus, the larger the amount of plastic strain, the greater will be the pressure required to suppress the void growth. In the case of the 0.004 pct C at 15.1 kbars and the spheroidized material at 21.3 kbars, it appears from the examination of the fracture appearance that no voids are present. This tends to contradict the above observation that the void suppression is progressive. A possible explanation is that the pressures are of a sufficient magnitude to suppress the void size to that below the resolution ability of the examination techniques utilized.

The suppression of the void growth by the pressure suggests a possible explanation for the increased ductility as a function of pressure in these materials. This agrees with the proposals of Bridgman[13] and Bobrowsky[10] and the observations of Pugh,[5] Davidson *et al.*[12] and Bulychev *et al.*[14]

The observed effects of pressure upon the fracture mechanisms may also suggest a possible reason for the similarity in the response of ductility to pressure for the 0.004 pct C and spheroidized materials as was shown in Fig. 2. First, the progressive increase in ductility with increasing pressure may be attributed to the progressive suppression of the void growth. Second, the fact that the form of the ductility-pressure relationship is the same for both the 0.004 pct C and spheroidized materials (linear) may be a manifestation of their having the same basic fracture propagation mechanism (void growth and coalescence). Finally, a possible reason for the decrease in slope of the ductility-pressure curves with increasing carbon content may be that as the number of cementite particles increases and the interparticle spacing decreases, the number of voids formed by the fracture of particles also increases and the growth required for coalescence decreases. Thus, it is likely that a higher pressure will be required to suppress the void growth and coalescence with increasing carbon content.

In the annealed 0.40, 0.83, and 1.1 pct C materials, the effects of pressure are to suppress void growth in pearlitic and free ferrite and to prevent cleavage of pearlite and hypereutectoid cementite. Although the fracture of the cementite is not prevented by the pressure, the fracture appears to convert from cleavage to shear. Furthermore, the pressure permits considerable plastic deformation of the cementite platelets in the pearlite prior to fracture. These observed effects of pressure on the various fracture mechanisms suggests why pressure enhances the ductility of the annealed 0.40, 0.83, and 1.1 pct C, materials.

The difference in the fracture mechanisms of the two types of material may also suggest an explanation for the nonlinear pressure ductility relationship and initially lower slope of the annealed 0.40, 0.83, and 1.1 pct C materials as compared to the annealed 0.004 pct C and spheroidized materials which exhibit a linear relationship, Fig. 2. Due to the close spacing of the cementite platelets in pearlite, there is an overlapping of the strain concentration fields of the voids initiated in the pearlitic ferrite. It is likely that a higher pressure is required to suppress this type of void growth as compared to the isolated voids in the 0.004 pct C and spheroidized materials. Also, the occurrence of cleavage in pearlite and hypereutectoid cementite requires a higher initial pressure for suppression. Finally, at higher pressures, the cementite platelets and/or hypereutectoid cementite become so extensively fragmented that the microstructure of the annealed materials tends to approach that of the spheroidized materials, *i.e.*, cementite particles in a ferrite matrix. This then may explain why the slopes of the ductility pressure curves for the annealed 0.40, 0.83, and 1.1 pct C materials increase with increasing pressure and tend to approach the slopes of the curves for the spheroidized materials.

CONCLUSIONS

1) Based upon optical and fractographic analysis, the principal effects of pressure upon the fracture mechanisms in annealed and spheroidized Fe-C materials are:
   a) To suppress the growth and coalescence of voids in ferrite.
   b) To retard the cleavage fracture of pearlite and hypereutectoid cementite.
   c) To impart some ductility to cementite and convert its fracture mode from cleavage to shear.
   d) To convert the macroscopic fracture mode from cup-cone, cleavage, or intergranular to a planar shear type.

2) The retardation by pressure of those fracture mechanisms resulting in low ductility suggests a possible explanation for the enhancement in ductility by pressure.

3) The observed structure sensitivity of the form of the ductility-pressure relationship to the amount, shape and distribution of cementite appears related to the differences in fracture propagation mechanisms and their modification by a superposed hydrostatic pressure.

REFERENCES

[1] P. W. Bridgman: *J. Appl. Phys.*, 1946, vol. 17, pp. 201-12.

[2] P. W. Bridgman: *Studies in Large Plastic Flow and Fracture*, 1st ed., pp. 32-50, 106-107, McGraw-Hill Book Co., New York, 1952.

[3] P. W. Bridgman: *J. Appl. Phys.*, 1953, vol. 24, pp. 560-70.

[4] H. Ll. D. Pugh: Proceedings of Conference on Irreversible Effects of High Pressure and Temperature on Materials, 1964, ASTM Special Technical Publication No. 374, pp. 68-140.

[5] H. Ll. D. Pugh: Recent Developments in Cold Forming, Bulleid Memorial Lecture Series vol. IIIB, pp. 4(1)-4(23), University of Nottingham Press, 1965.

[6] B. I. Beresnev, L. F. Vereshchagin, Y. N. Ryabinin, and L. D. Livshits: *Some Problems in Large Plastic Deformation in Metals Under High Pressure*, Pergamon Press, 1963.

[7] L. D. Livshits, Y. N. Ryabinin, and B. I. Beresnev: *Zh. Tekh. Fiz.*, 1965, vol. 35, pp. 348-54.

[8] T. Pelczynski: *Arch. Hutnictwa*, 1962, vol. 7(1), pp. 3-13.

[9] S. I. Ratner: *Zh. Tekh. Fiz.*, 1949, vol. 19(3), pp. 408-11.

[10] A. Bobrowsky and E. A. Stack: Proc. AIME Conference on Metallurgy at High Pressures and High Temperatures, Gordon and Breach Science Publishers, New York, 1964.

[11] M. Brandes: *Prace. Inst. Mech. Precyzncy*, 1962, vol. 10, pp. 1-17.

[12] T. E. Davidson, J. C. Uy, and A. P. Lee: *Acta Met.*, 1966, vol. 14, pp. 937-48.

[13] P. W. Bridgman: *Research (London)*, 1949, vol. 2, pp. 550-55.

[14] D. K. Bulychev, B. I. Beresnev, M. G. GayduKou, Y. D. Martynov, K. P. Rodionov, and Y. N. Ryabinin: *Fiz. Metal. Metalloved.*, 1964, vol. 18, no. 3, pp. 437-42.

[15] J. R. Galli and P. Gibbs: *Acta Met.*, 1964, vol. 12, pp. 775-78.

[16] T. E. Davidson and G. S. Ansell: *ASM Trans. Quart.*, 1968, vol. 61, no. 2, pp. 242-54.